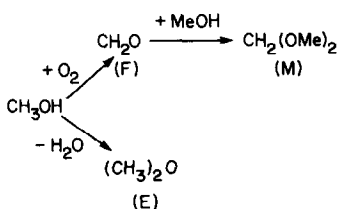# A Structure-Sensitive Oxidation Reaction: Methanol on Molybdenum Trioxide Catalysts

The vapor phase reaction of diluted methanol–oxygen mixtures at 200–300°C and 1 atm was catalyzed on different preparations of pure (unsupported) molybdenum trioxide. At low conversion levels, formaldehyde (F) and its acetal (M) (oxidation), and dimethylether (E) (dehydration) are the only reaction products:

$$CH_3OH \begin{array}{c} \xrightarrow{+O_2} CH_2O \xrightarrow{+MeOH} CH_2(OMe)_2 \\ (F) \qquad\qquad (M) \\ \xrightarrow{-H_2O} (CH_3)_2O \\ (E) \end{array}$$

We have shown previously (1) that the two polymorphic crystalline forms of MoO_3, hexagonal and orthorhombic, have quite different catalytic properties. Orthorhombic MoO_3 has a low activity but a high selectivity to oxidation products (F) and (M); hexagonal MoO_3, highly active, is less selective for oxidation, and more for dehydration to (E). In the present note, we show that various samples of crystalline orthorombic MoO_3 present large differences of selectivity when the relative extent of the different exposed crystal faces is changed: the methanol oxidation is therefore a structure-sensitive catalytic reaction on MoO_3.

The catalytic measurements have been performed in a continuous flow isothermal reactor with on-line chromatographic analysis of feed and product gases. A standard test mixture,

$$MeOH/O_2/He : 8.2/19.7/72 \text{ (molar)},$$
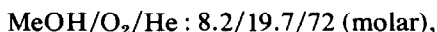
was fed to the reactor at 291°C and 1 atm, the flow rate being such that methanol conversion did not exceed 5%.

The measured selectivities to formaldehyde (S_F), methylal (S_M), and ether (S_E), and the reaction rate A ($M/h \cdot m^2$) are "initial values" calculated on the number of moles MeOH converted to these products.

Very pure (Merck) MoO_3 was submitted to sublimation; the collected crystals, flat needles (Fig. 1) 40 μm thick (e) were separated through appropriate sieves in 4 different fractions (S_1, S_2, S_3, S_4) according to their size (length L and width l). A fifth sample (C) was prepared from the same MoO_3 batch, simply calcined 3 h at 710°C under O_2, lightly ground to separate the individual microcrystals, and sieved. Crystal shapes and sizes were similar to those of sample S_1 above.

A statistical study of microphotographs made it possible to calculate for each sample, the average dimensions (L, l, e), the surface area (S) and the percentage of the different exposed crystal faces: basal (010), side (100), apical (001) + (101) (Fig. 1). Crystallographic orientations were found by electron diffraction patterns (see Tables 1 and 3).
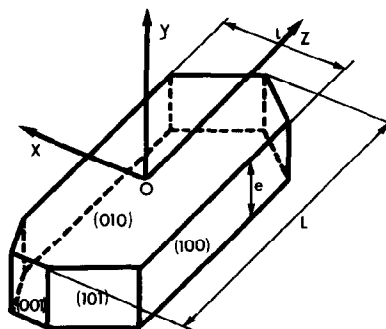
Due to the low surface area and activities

FIG. 1. Orthorhombic MoO_3 crystallite and exposed faces. L, length; basal planes (010); l, width; side planes (100); e, thickness; apical planes (001) + (101).

TABLE 1

Selectivities and Percentages of Exposed MoO₃ Faces

Catalyst (ref)	(010) b faces (%)	(100) s faces (%)	(001) + (101) a faces (%)	S_F (%)	S_M (%)	S_E (%)
S_1	69.0	27.6	3.4	65.0	27.1	7.9
S_2	77.6	19.4	3.0	76.7	15.7	7.6
S_3	86.6	11.6	1.8	83.7	11.0	5.3
S_4	90.3	8.0	1.7	89.0	8.0	3.0
C	69.2	29.1	1.7	67.2	28.6	4.2

of these catalysts, large amounts (~2 g) of each sample were needed in catalytic measurements.

The results are as follows. The initial selectivities to formaldehyde (F), methylal (M), and dimethyl ether (E) show large changes with the percentages of exposed crystal faces (Table 1). Selectivities to formaldehyde, methylal and ether clearly follow respectively the percentages of basal (010), side (100), and apical (001) + (101) faces.

A quantitative check of these statements is possible; let us define the intrinsic activities of each face for each product as in the square matrix of Table 2. The plots of S_E/S_M vs %b/%s (Fig. 2) and of S_E/S_F vs %a/%b (Fig. 3) are straight lines passing through the origin; as a consequence (see Appendix) all terms except diagonal ones in the matrix of Table 2 are zero:

$$A_M{}^b = A_E{}^b = A_F{}^s = A_E{}^s = A_F{}^a = A_M{}^a = 0$$

and the slopes of the two lines (Figs. 2 and 3) indicate:

TABLE 2

Definition of Intrinsic Activities

Product	Face		
	basal (010)	side (100)	apical (001) + (101)
Formaldehyde	$A_F{}^b$	$A_F{}^s$	$A_F{}^a$
Methylal	$A_M{}^b$	$A_M{}^s$	$A_M{}^a$
Dimethyl ether	$A_E{}^b$	$A_E{}^s$	$A_E{}^a$

$$A_F{}^b/1 = A_M{}^s/1 = A_E{}^a/2.5.$$

Absolute values of intrinsic activities for each face may now be calculated since surface area are known (Table 3).

Values of activities should be independent of crystal size for each face. Due to the approximate values of surface areas (averaging process) the dispersion of data is rather high, with mean values of:

$$A_F{}^b \cong A_M{}^s \cong 3 \times 10^{-3} \; M/h \cdot m^2,$$
$$A_E{}^a \cong 8 \times 10^{-3} \; M/h \cdot m^2.$$

Within the expected margin of error, the intrinsic activity of each face is the same for all catalysts, including the sample C (not sublimed).
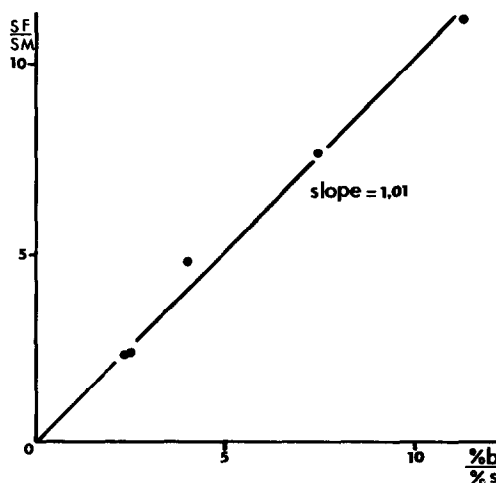

FIG. 2. Ratios of formaldehyde and methylal selectivities (S_F/S_M) vs ratios of basal and side faces $(\%b/\%s)$.
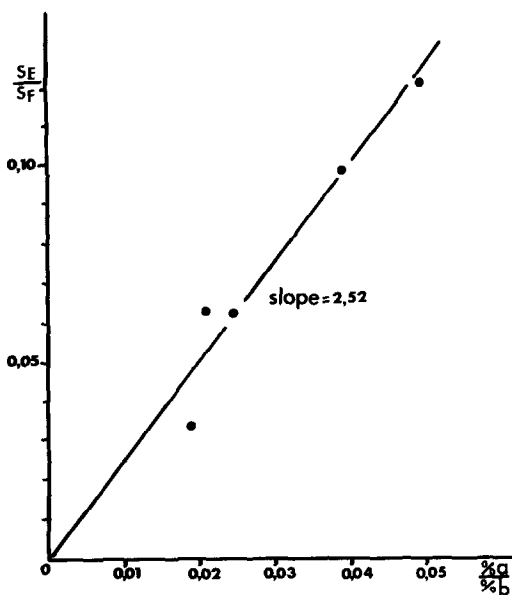
FIG. 3. Ratios of dimethyl ether and formaldehyde selectivities (S_E/S_F) vs ratios of apical and basal faces (%a/%b).

The results show that the structure sensitivity of methanol oxidation on orthorhombic crystals of MoO_3 is due to catalytic specificity of the different exposed faces. We have found similar effects in ethanol oxidation (2) where the products are acetaldehyde (oxidation), and diethyl ether and ethylene (dehydration). From the known structure of MoO_3 (3) we inferred that (010) faces (cleavage plane) carry active centers for dehydrogenation (Mo—O groups), while (100) faces present the same groups plus Lewis acid centers active for dehydration. This picture is consistent with the present results. Formaldehyde is produced on the (010) face by oxidative dehydrogenation; the acetal formation, which requires dehydrogenating and dehydrating centers, takes place on the bifunctional (100) face:

$$3CH_3OH + \tfrac{1}{2}O_2 \rightarrow CH_2(OCH_3)_2 + 2H_2O.$$

The identification of oxidative dehydrogenation centers with protruding Mo=O groups has been proposed by several groups of workers (4, 5), and the presence of Lewis acid centers on MoO_3 demonstrated by ir studies (6).

Structure sensitivity of MoO_3 (supported on graphite) was also reported for catalytic oxidation of propylene (7).

As MoO_3 is the basic ingredient of many oxidation catalysts, this new factor of selectivity could explain particular promoter or support effects in such systems as MoO_3–TiO_2 (8) (benzene oxidation to maleic anhydride) or Bi–Mo–O (9) (butene oxidation to butadiene).

In any event, it is clear that the concept of structure sensitivity, introduced by Boudart (10) in metal-catalyzed hydrogen–hydrocarbon reactions, is now extended to oxide-catalyzed oxidation reactions.

APPENDIX

Each intrinsic activity A_F, A_M, A_E may be expressed in terms of a matrix (Table 2);

$$A_F = \%b\,A_F{}^b + \%s\,A_F{}^s + \%a\,A_F{}^a,$$
$$A_M = \%b\,A_M{}^b + \%s\,A_M{}^s + \%a\,A_M{}^a,$$
$$A_E = \%b\,A_E{}^b + \%s\,A_E{}^s + \%a\,A_E{}^a,$$

TABLE 3

Average Crystal Sizes, Surface Areas, and Activities of the Different Crystal Faces

Catalyst	L (mm)	l (mm)	e (mm)	S (m²/g)	$A_F{}^b$ (mM/h · m²)	$A_M{}^s$ (mM/h · m²)	$A_E{}^a$ (mM/h · m²)
S_1	0.82	0.10	0.04	0.0154	2.3	2.4	5.6
S_2	1.05	0.16	0.04	0.0137	3.1	2.5	7.9
S_3	1.92	0.30	0.04	0.0123	2.6	2.6	8.1
S_4	2.14	0.45	0.04	0.0118	5.0	5.1	8.9
C	0.6	0.1	0.04	0.0156	3.4	3.4	8.7

and the total activity per unit surface area is:

$$A = A_F + A_M + A_E.$$

Selectivities are, by definition:

$$S_F = A_F/A; \quad S_M = A_M/A; \quad S_E = A_E/A.$$

Therefore, the ratios of selectivities are:

$$S_F/S_M = A_F/A_M: \quad S_E/S_F = A_E/A_F.$$

Consider the experimental plot of Fig. 2. $S_F/S_M \cong (\%b/\%s)$ (slope 1.01) compared with the theoretical expression of $S_F/S_M = A_F/A_M$ indicates that:

$$A_F^s = A_F^a = 0,$$
$$A_M^b = A_M^a = 0$$

$$\text{and} \quad A_F^b/A_M^s \cong 1. \quad (1)$$

Consider also the experimental plot of Fig. 3. $S_E/S_F \cong 2.5 \ (\%a/\%b)$ (slope 2.52) compared with the theoretical expression $S_E/S_F = A_E/A_F$ indicates that:

$$A_E^b = A_E^s = 0,$$
$$A_F^s = A_F^a = 0$$

$$\text{and} \quad A_E^a/A_F^b \cong 2.5. \quad (2)$$

As a supplementary verification, the curves S_F/S_E vs $(\%b/\%a)$ and S_M/S_E vs $(\%s/\%a)$ have been found to be straight lines passing through the origin, with slopes close to 0.4:

$$A_F^b/A_E^a = A_M^s/A_E^a = 0.4. \quad (3)$$

This is consistent with the above results (1) and (2). As a consequence, the matrix of activities (Table 2) reduces to:

	b	s	a
F	A_F^b	0	0
M	0	A_M^a	0
E	0	0	A_E^a

REFERENCES

1. Tatibouët, J. M., and Germain, J. E., C. R. Acad. Sci. Paris. Ser. C 290, 321 (1980).
2. Tatibouët, J. M., and Germain, J. E., J. Chem. Research (S) 268 (1981); (M) 3070 (1981).
3. Kihlborg, L., Ark. Kemi 21, 357 (1963).
4. Trifirò, F. Notarbartolo, S., and Pasquon, I. J. Catal. 22, 324 (1971).
5. Weiss, F., Marion, J., Metzger, J., and Cognion, J. M., Kinet. Katal. 14, 45 (1973).
6. Bianchi, D., Tatibouët, J. M., Germain, J. E., and Teichner, S. J., in "5ème Colloque Franco–Soviétique sur la Catalyse, Lille 1980."
7. Volta, J. C., Desquesnes, W., Morawek, B. and Tatibouët, J. M., in "Proceedings, 7th International Congress on Catalysis, (Tokyo, 1980), p. 1398. Elsevier, Amsterdam, 1981.
8. Déchelette, J., and Germain, J. E., Bull. Soc. Chim. Fr., 874 (1976).
9. Batist, P. A., Kapteijns, C. J., Lippens, B. C., and Schuit, G. C. A., J. Catal. 7, 33 (1967).
10. Boudart, M., in "Advances in Catalysis," Vol. 20, p. 153. Academic Press, New York, 1969.

J. M. Tatibouët
J. E. Germain

Laboratoire de Catalyse Organique
L.A. 231 CNRS
ESCIL, Université Claude Bernard (Lyon I)
43 Boulevard du 11 Novembre 1918,
69622 Villeurbanne Cédex, France